Research Article

Diffusion tensor imaging of the hippocampus reflects the severity of hippocampal injury induced by global cerebral ischemia/reperfusion injury

https://doi.org/10.4103/1673-5374.322468

Date of submission: November 24, 2020

Date of decision: March 25, 2021

Date of acceptance: May 11, 2021

Date of web publication: August 30, 2021

Wen-Zhu Wang[1, 2], Xu Liu[3], Zheng-Yi Yang[4], Yi-Zheng Wang[1], Hai-Tao Lu[1, *]

Graphical Abstract *Change of diffusion tensor imaging in hippocampus reflects hippocampal injury severity induced by global cerebral ischemia/reperfusion injury*

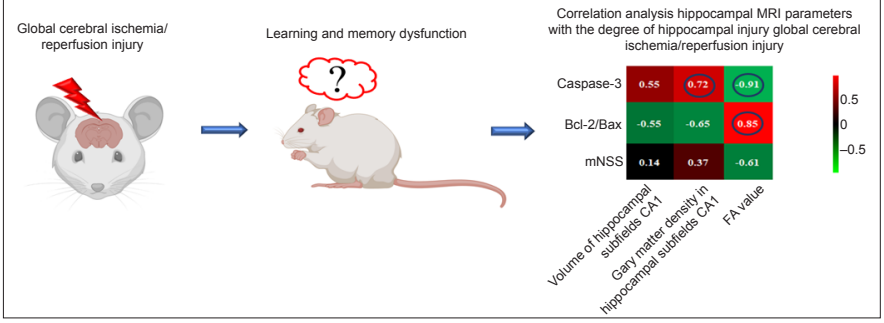

Abstract

At present, predicting the severity of brain injury caused by global cerebral ischemia/reperfusion injury (GCI/RI) is a clinical problem. After such an injury, clinical indicators that can directly reflect neurological dysfunction are lacking. The change in hippocampal microstructure is the key to memory formation and consolidation. Diffusion tensor imaging is a highly sensitive tool for visualizing injury to hippocampal microstructure. Although hippocampal microstructure, brain-derived neurotrophic factor (BDNF), and tropomyosin-related kinase B (TrkB) levels are closely related to nerve injury and the repair process after GCI/RI, whether these indicators can reflect the severity of such hippocampal injury remains unknown. To address this issue, we established rat models of GCI/RI using the four-vessel occlusion method. Diffusion tensor imaging parameters, BDNF, and TrkB levels were correlated with modified neurological severity scores. The results revealed that after GCI/RI, while neurological function was not related to BDNF and TrkB levels, it was related to hippocampal fractional anisotropy. These findings suggest that hippocampal fractional anisotropy can reflect the severity of hippocampal injury after global GCI/RI. The study was approved by the Institutional Animal Care and Use Committee of Capital Medical University, China (approval No. AEEI-2015-139) on November 9, 2015.

Key Words: brain-derived neurotrophic factor; diffusion tensor imaging; fractional anisotropy value; global cerebral ischemia/reperfusion injury; hippocampus; TrkB

Chinese Library Classification No. R446.8; R741; [R445.6]

Introduction

The brain is the organ most sensitive to ischemia and hypoxia. Five to twenty minutes after respiratory or cardiac arrest, primary injury occurs because of ischemia and hypoxia, as well as delayed cell death even after restoring blood flow under certain conditions. This further aggravates structural and functional brain damage, which is known as global cerebral ischemia/reperfusion injury (GCI/RI) (Kalogeris et al., 2012). GCI/RI causes ischemic tissue damage and excitotoxicity, which increases free radical release, initiates apoptosis (through caspase-family proteins) (Jakaria et al., 2018).

Memory loss is the earliest and most prominent clinical manifestation. Furthermore, a persistent vegetative state may occur in severe cases (Fujioka et al., 1994). Clinical diagnosis, severity, and prognosis of brain injury after ischemia-reperfusion depend primarily on medical history, clinical signs and symptoms, and routine electrophysiological and imaging examination results. However, there are no objective and uniform standards that directly reflect brain injury, particularly for measuring indices associated with cognitive (learning and memory) impairments.

BDNF is an essential factor for promoting nerve growth and regeneration that exerts its biological effects by binding to its receptor, tyrosine receptor kinase B (TrkB). BDNF is involved in regulating neuronal structure—including synapse generation, maintenance, expansion, and modification—and neuronal function—including neurotransmission, receptor activity, and

[1]China Rehabilitation Science Institute, School of Rehabilitation Medicine, Capital Medical University, Beijing Bo'ai Hospital, China Rehabilitation Research Center, Beijing, China; [2]Beijing Key Laboratory of Neural Injury and Rehabilitation, Beijing, China; [3]Department of Rehabilitation Medicine, Beijing Friendship Hospital, Capital Medical University, Beijing, China; [4]Brainnetome Center, Institute of Automation, Chinese Academy of Sciences, Beijing, China

***Correspondence to:** Hai-Tao Lu, PhD, 13051760807@163.com.

https://orcid.org/0000-0002-1775-9780 (Hai-Tao Lu)

Funding: *This study was supported by the Fundamental Research Funds for Central Public Welfare Research Institute of China, Nos. 2015CZ-36 (to HTL) and 2019CZ-7 (to WZW).*

How to cite this article: *Wang WZ, Liu X, Yang ZY, Wang YZ, Lu HT (2022) Diffusion tensor imaging of the hippocampus reflects the severity of hippocampal injury induced by global cerebral ischemia/reperfusion injury. Neural Regen Res 17(4):838-844.*

the promotion of dendritic and axonal growth (Chen et al., 2018). Thus, it is crucially involved in learning and memory plasticity. Under normal and pathological conditions, BDNF and TrkB expression in the central and peripheral nervous system is affected by numerous factors. The hippocampus is the brain region most directly in control of learning and memory function. As a high-affinity BDNF receptor, TrkB is both pre- and post-synaptically expressed (Callaghan and Kelly, 2012). The presence of BDNF-TrkB can increase neuronal plasticity in the hippocampus and regulate learning and memory at the cellular level (Li et al., 2018).

Microstructural damage to the hippocampus correlates with memory impairment (Planche et al., 2017). Moreover, it is vulnerable during GCI/RI and as mentioned, contains abundant BDNF and TrkB. Diffusion tensor imaging (DTI) is an imaging technique that is sensitive to microstructural damage in the hippocampus (Sampaio-Baptista and Johansen-Berg, 2017). BDNF in brain tissue enters the blood by crossing the blood-brain barrier. Blood BDNF levels are correlated with neurological function after brain injury, and serum BDNF levels in patients with cerebral ischemia are thought to be positively correlated with neurological functional recovery (Zhou et al., 2011). However, Béjot et al. (2011) reported no association of circulating BDNF levels with stroke severity. Thus, whether circulating BDNF levels correlate with neurological function after cerebral ischemia-reperfusion injury remains an open issue.

The hippocampal CA1 subfield can become obviously damaged even after a short ischemic period because of its selective vulnerability to ischemic and hypoxic factors. Microstructural changes in hippocampal subfields have been reported to lead to age-related memory decline (Radhakrishnan et al., 2020). Changes in gray matter density and volume in the hippocampus are associated with reduced cognitive performance in normal brain aging (Fletcher et al., 2018; Herrmann et al., 2019). Moreover, increased hippocampal BDNF expression can improve learning and memory (Kowiański et al., 2018). However, whether blood BDNF and TrkB levels after GCI/RI correlate with pathological microstructure, gray matter density, or other manifestations of clinical damage to the hippocampus (especially damage in the ischemia-vulnerable area) is an open question. Additionally, whether any correlation of BDNF or TrkB levels changes depending on where measurements are taken (plasma or hippocampus) remains unknown. The aim of this study was to explore the clinical application value of using DTI with plasma BDNF measurements to predict learning and memory impairment caused by GCI/RI.

Although hippocampal microstructure, BDNF, and TrkB levels are closely related to nerve injury and the repair process after GCI/RI, whether these indicators can reflect the severity of such hippocampal injury remains unknown. To address this issue, this study used the four-vessel occlusion method to simulate GCI/RI. Compared with three-vessel occlusion, Pulsinelli's four-vessel occlusion is a better model for mimicking the clinical situation of cardiac arrest (Wang et al., 2019). The expression of apoptosis-related proteins, BDNF, and TrkB in the hippocampus was determined at different time points after injury, as was plasma BDNF and TrkB expression levels, in order test the correlation between BDNF and TrkB expression in both the hippocampus and in the blood with hippocampal damage following GCI/RI. Because individual hippocampal subregions are vulnerable to cerebral ischemia, magnetic resonance imaging (MRI) technology was used to investigate the density and volume of gray matter in the CA1, CA2, CA3, and dentate gyrus (DG) subfields to gain a more comprehensive understanding of the damage to each hippocampal subregion after GCI/RI.

Materials and Methods

Experimental animals

We purchased experimental specific-pathogen-free male Sprague-Dawley rats weighing 250–300 g (7 weeks of age, *n* = 120) from Beijing Vital River Laboratory Animal Technology Co., Ltd., license No. SCXK (Beijing) 2012–0001. The animals were raised in the animal barrier laboratory of the Chinese Institute of Rehabilitation Science. Rats were housed in a temperature-controlled room (23 ± 1°C) with 50–70% humidity under a 12-hour light/dark cycle. Access to food and water was ad libitum. The study was approved by the Institutional Animal Care and Use Committee of Capital Medical University (approval No. AEEI-2015-139) on November 9, 2015. The rats were housed in groups of three in standard polypropylene cages. The rats were randomly divided into sham-operated (sham) and GCI/RI model (model) groups using the random number-table method. All surgeries were under anesthesia with intraperitoneal injection of 60 mg/kg pentobarbital sodium (Sigma-Aldrich, St. Louis, MO, USA).

Establishment of the GCI/RI model

The rat model was established using the modified Pulsinelli's four-vessel occlusion method. Briefly, bilateral vertebral arteries were electrocoagulated while bilateral carotid arteries were clamped using non-invasive vascular clamps for 20 minutes and subsequently released (Wang et al., 2019). In the sham group, the bilateral vertebral and common carotid arteries were not electrocoagulated or clamped. The groups were not different in any other way.

Modified neurological severity score

Modified neurological severity scores (mNSS) were obtained before surgery and on days 3, 7, and 14 after GCI/RI. The mNSS is an 18-point scoring system that includes movement, sensation, balance, and reflection (Wang et al., 2019). A higher score means more severe injury. We used the double-blind method for the scoring to achieve the final average value. The animals were subjected to the conditions mentioned above for a week before starting the experiment. Mice with a score above 1 before surgery were eliminated (normal score = 0).

Morris water maze tests

The Morris water maze is used to test memory in mice and rats. We used a Morris water maze that had a circular water tank (160 cm diameter) and a pool divided into four quadrants (model number XR-XM101, Friends Honesty Life Sciences Co., Ltd., Hong Kong, China). Each rat was trained to find a platform three times per day for five consecutive days. For each rat, the platform was placed in the same location each time (but not the same location between rats), and the quadrant it was in was called the goal quadrant. On the spatial navigation test, once the rat found the submerged platform, it was allowed to stay there for 10 seconds and the time taken to leave the platform was recorded. On day 5, the platform was removed followed by a space exploration test. During the test, rats were allowed 120 seconds to search for the hidden platform. We recorded the time that they remained in the goal quadrant and the number of times the platform was crossed.

MRI

MRI scanning

All the rats underwent MRI scans on days 3, 7, and 14 after GCI/RI using a 7.0 T MRI scanner (PharmaScan, Bruker Biospin, Rheinstetten, Germany) at the Small Animal Magnetic Resonance Laboratory of Capital Medical University. The brains were scanned with T2WI and DTI sequences using the following parameters. (1) T2: rapid imaging with refocused-echo sequence; slice thickness: 0.3 mm; gap: 0 mm; slices: 90; repetition time = 10,700 ms; echo time = 36 ms; flip angle = 180°; phase encoding direction: left to right; number of superimposed layers: 4; (2) DTI: echo-planar imaging, single-

shot, spin-plane echo-imaging sequence; slices: 60; repetition time = 15,000 seconds; echo time = 22.4 ms; flip angle = 90°; *b* value 1 = 0; *b* value 2 = 1000 s/mm^2; 30 gradient directions; phase encoding direction: left to right; number of superimposed layers: 1.

Voxel-based morphometry analysis

Voxel-based morphometry was performed to analyze the rat-brain structural MRI (Ashburner and Friston, 2005; Wang et al., 2020). The "segment" function in SPM12 software (Ashburner, 2012) based on the MATLAB 9.3 platform (MathWorks Inc., Natick, MA, USA) was used to correct intensity inhomogeneity in images, as well as to perform spatial standardization and tissue segmentation. Images were divided into gray matter, white matter, cerebrospinal fluid, and non-brain voxels. The voxel size after segmentation was 0.125 mm × 0.125 mm × 0.125 mm. Modulated tissue maps of gray matter were generated using the Jacobian determinant of the deformation field obtained in the normalization process to encode the expansion or contraction of voxels. Therefore, the tissue volume of each voxel was preserved in the modulated tissue maps. A Gaussian kernel with a full-width at half maximum of 0.3 mm was used for smoothing to increase the parameter validity and reduce the spatial noise caused by registration errors.

DTI data processing

Two researchers collected DTI data, selected slices with the largest hippocampal area on coronal brain MRI images, and chose the bilateral hippocampus as the region of interest. The fractional anisotropy (FA) value of the hippocampal region of interest was determined as the average value of both sides.

Nissl staining

At 3, 7, and 14 days after reperfusion, six rats in each group were perfused and fixed with paraformaldehyde. Subsequently, the brains were collected, placed in 4% paraformaldehyde solution, and stored in a 4°C refrigerator for 24 hours. After conventional dehydration and embedding, hippocampal tissue was prepared into paraffin blocks, sliced into 3-μm sections, and subjected to Nissl staining (Wang et al., 2020). Subsequently, the sections were stained using aniline blue staining solution for 5–10 minutes, washed with distilled water, cleared, and mounted.

Serial coronal slides of the paraffin-embedded hippocampal tissue blocks were obtained at intervals of six sections. The slides were scanned using a tissue cytometer (Tissue Gnostics, Vienna, Austria) with a 20× objective lens. The number of surviving neurons in the intact membrane and the nuclei in the CA1 hippocampal subfield were manually calculated in three non-overlapping areas (220 × 350 μm^2).

Western blot assay

The rats were decapitated followed by rapid harvesting of hippocampal tissue and weighing. Cell lysate buffer was added for homogenization. Subsequently, the homogenate was thoroughly centrifuged followed by protein electrophoresis. Extracted proteins were separated using 10% sodium dodecyl sulfate-polyacrylamide gel electrophoresis followed by electroblotting onto a polyvinylidene fluoride membrane (Millipore, Billerica, MA, USA). Next, the membrane was blocked for 1 hour at room temperature using 5% skim milk powder diluted in Tris Buffered Saline with Tween-20. The membrane was incubated with rabbit anti-Caspase-3 (Cat# 9662, 1:1000, Cell Signaling Technology, Danvers, MA, USA), rabbit anti-BDNF (Cat# ab108319, 1:1000, Abcam, Cambridge, MA, USA), rabbit anti-TrkB (Cat# 4606S, 1:1000, Cell Signaling Technology, Danvers, MA, USA), rabbit anti-Bax (Cat# 2772S, 1:1000, Cell Signaling Technology), β-actin (Cat# 4970, 1:1000, Cell Signaling Technology) and rabbit anti-Bcl2 (Cat# 3498, 1:1000, Cell Signaling Technology) overnight at 4°C. Subsequently, the membrane was incubated using goat anti-rabbit antibody (Cat#31460, 1:5000, Thermo Scientific, Waltham, MA, USA) for 2 hours at 37°C to allow color development. Scanning was performed using a multifunctional laser scanning imaging system (Bio-Rad Laboratories, Inc., Hercules, CA, USA). The intensity of blots was quantified with ImageJ software (National Institutes of Health, Bethesda, MD, USA).

Enzyme-linked immunosorbent assay

Blood samples (0.5 mL/rat) were collected from the rats' jugular veins in an anticoagulant tube. All samples were allowed to stand for 1.5 hours at room temperature, then centrifuged for 15 minutes at 1000 × *g* until samples were clear. The samples were collected under sodium pentobarbital anesthesia just before sacrifice. Plasma was stored at –80°C until BDNF and the TrkB receptor were assayed using enzyme-linked immunosorbent assays (ELISAs) for BDNF (Rat BDNF ELISA kit, Rrigo Biolaboratories Corp., Hsinchu, Taiwan, China) and TrkB (Rat TrkB ELISA kit, Dogesce, Beijing, China), respectively. These ELISA kits use the Sandwich-ELISA method (Elfving et al., 2010). The micro ELISA plate provided in the kits was precoated with an antibody specific to rat BDNF or TrkB. Standards or samples were added to the appropriate micro ELISA plate wells and combined with the specific antibody.

Statistical analysis

The sample size was calculated using PASS 15.0 software (NCSS, Kaysville, UT, USA). All statistical analyses were performed using SPSS 22.0 software (IBM Corp., Armonk, NY, USA). Statistical graphs were generated using GraphPad Prism7 software (GraphPad Software Inc., La Jolla, CA, USA). Data are represented as mean ± standard deviation (SD) and were tested for normal distribution and variance homogeneity. The statistical significance between-groups was assessed with a Student's *t*-test and among multiple groups by a one-way analysis of variance (ANOVA) with subsequent least-significant difference multiple comparison tests if appropriate. Calculations of the Pearson correlation coefficient were performed using SPSS 22.0 software. Heat maps were created in EXCEL (Microsoft Corporation, Redmond, WA, USA). The significance level was set at $P = 0.05$.

Results

The mNSS decreases after GCI/RI

The mNSS was higher in the model group than in the sham group on days 3, 7, and 14 (3 days: $t = –17.678$, $P < 0.01$; 7 days: $t = –8.000$, $P < 0.01$; 14 days: $t = –2.828$, $P < 0.05$), and gradually decreased with time ($F_{(2,24)} = 107.918$; $P < 0.001$; **Figure 1A**). Analysis showed that the mNSS scores at day 3 were higher than those on days 7 or 14 ($P < 0.001$), and the mNSS scores on days 7 and 14 continued to decline.

Learning and memory function decreases after GCI/RI

The swimming paths of the rats in the sham group were smoother than those in the other three groups (**Figure 1B**). On the spatial navigation test, the escape latency was greater in the model group than in the sham group for three consecutive days starting from day 7 (2 days: $t = –3.137$, $P < 0.01$; 3 days: $t = –5.509$, $P < 0.01$; 4 days: $t = –7.628$, $P < 0.01$) and from day 14 (2 days: $t = –6.195$, $P < 0.01$; 3 days:, $t = –13.561$, $P < 0.01$; 4 days: $t = –15.305$, $P < 0.01$; **Figure 1C**). Moreover, time spent in the goal quadrant was less in the model group than in the sham group on days 7 and 14 (day 7: $t = 37.484$, $P < 0.01$; day 14: $t = 21.934$, $P < 0.01$; **Figure 1D**).

Hippocampal CA1 and CA3 volumes increase after GCI/RI

Paired *t*-tests were used to compare the volumes of the hippocampal subfields (CA1, CA2, CA3 and DG) in sham and model groups on days 3, 7, and 14 after reperfusion. The results showed that CA1 and CA3 volumes were greater

in the model group than in the sham group on day 3 after reperfusion (CA1: t = −2.874, P < 0.05; CA3: t = −3.263, P < 0.05; **Figure 2A** and **B**); however, no between-group differences were found on days 7 (CA1: t = −2.049, P = 0.096; CA3: t = −1.259, P = 0.264) or 14 (CA1: t = −0.834, P = 0.442; CA3: t = −0.578, P = 0.588; **Figure 2A** and **B**). We found no between-group differences in the CA2 or DG hippocampal subregions at any of the post-reperfusion time points (CA2-3d: t = −2.268, P = 0.073; CA2-7d: t = −0.372, P = 0.725; CA2-14d: t = −1.204, P = 0.283; DG-3d: t = −0.408, P = 0.700; DG-7d: t = −0.372, P = 0.725; DG-14d: t = −1.435, P = 0.211).

Gray matter density of hippocampal subregions increase after GCI/RI

Paired *t*-tests were used to compare the gray matter density of the hippocampal subfields (CA1, CA2, CA3 and DG) between sham and model groups on days 3, 7, and 14 after reperfusion. Analysis showed that gray matter density in the CA1 and CA2 regions were higher in the model group than in the sham group on days 3 (CA1: t = 7.715, P < 0.05; CA2: t = −43.301, P < 0.01), 7 (CA1: t = −9.007, P < 0.05; CA2: t = 102.191, P < 0.01), and 14 after reperfusion (CA1: t = −5.966, P < 0.05; CA2: t = −13.856, P < 0.01; **Figure 2C** and **D**). Moreover, we found significant differences in the gray matter density of the CA3 and DG regions between sham and model groups on day 14 (CA3: t = −9.526, P < 0.05; DG: t = −8.227, P < 0.05), but not at the other time points (CA3-3d: t = −2.155, P = 0.164; CA3-7d: t = −3.959, P = 0.058; DG-3d: t = −1.516, P = 0.269; DG-7d: t = 1.155, P = 0.368; **Figure 2E** and **F**).

Hippocampal FA value decreases after GCI/RI

We used DTI to measure the FA value of the hippocampus in the sham and model groups on days 3, 7 and 14 after reperfusion injury. An independent-samples *t*-test was used to compare the FA values between groups on each day. We found that on each of the three days, FA values were lower in the model group than in the sham group (3 days: t = 6.598, P < 0.01; 7 days: t =7.843, P < 0.01; 14 days: t = 5.169, P < 0.01; **Figure 2G**).

Delayed hippocampal neuronal cell death after GCI/RI

Caspase-3 expression and Bcl-2/Bax levels in the hippocampus determined by western blot assay

Caspase-3 expression in hippocampus on days 3 (t = −4.342, P = 0.012), 7 (t = −12.487, P = 0.006), and 14 (t = −4.21, P = 0.014) after reperfusion was significantly higher than that in the sham group. Moreover, hippocampal Bcl-2/Bax levels were significantly lower in the model group than in the sham group on each day (day 3: t = 13.920, P < 0.01; day 7: t = 8.922, P < 0.05; day 14: t = 12.529, P < 0.01; **Figure 3A–C**).

Nissl staining

In the sham group, CA1 neurons were large and round with uniformly colored cytoplasm. Further, the Nissl bodies around the cytoplasm were uniformly blue with normal morphology and a full shape (**Figure 4A**). Conversely, on days 3, 7, and 14 after injury, CA1 neurons in the model group were deformed and showed karyopyknosis, blurry cell outlines, loose arrangement, and enlarged spaces. Moreover, very few neurons showed normal morphology (**Figure 4A–H**). CA1 neurons were counted under high magnification. The results revealed fewer hippocampal neurons in the model group on days 3 (t = 11.215, P < 0.01), 7 (t = 10.56, P < 0.01), and 14 (t = 12.411, P < 0.01) after reperfusion than in the sham group (**Figure 4I**).

Change in BDNF and TrkB levels in the hippocampus and plasma after GCI/RI

BDNF and TrkB levels in the hippocampus

BDNF expression 3 days (t = −4.195, P < 0.05) after reperfusion was significantly higher in the model group than in the sham group. BDNF expression 7 days (t = 3.944, P < 0.05) and 14 days (t = 2.697, P < 0.05) after reperfusion was significantly lower in the model group than in the sham group (**Figure 3A** and **D**). TrkB expression was lower in the model group than in the sham group on all 3 time points (day 3: t = 42.203, P < 0.01; day 7: t = 39.299, P < 0.01; day 14: t = 11.462, P < 0.05; **Figure 3A** and **E**).

BDNF and TrkB levels in plasma

BDNF and TrkB in plasma were detected by ELISA. Compared with the sham group, the model group had significantly higher plasma BDNF content on day 3 (t = −3.196, P < 0.05), but significantly lower plasma BDNF content on days 7 and 14 (7 days: t = 147.105, P < 0.001; 14 days: t =3.927, P < 0.05; **Figure 5A**). The pattern of plasma BDNF content after reperfusion was consistent with that of hippocampal BDNF expression as determined by western blotting.

Plasma TrkB content in the model group on days 3 and 14 was significantly higher than that in the sham group (3 days: t = 4.508, P < 0.05; 14 days: t = −9.608, P < 0.05). There was no between-group difference in plasma TrkB content on day 7 after reperfusion (t = 3.521, P = 0.072; **Figure 5B**).

Correlation between BDNF and TrkB levels with other indicators

We performed linear correlation analyses between BDNF and TrkB content (hippocampal and plasma) with the mNSS, mean gray matter density of CA1, CA1 volume, FA value, hippocampal Caspase-3, Bcl-2/Bax ratio, and BDNF expression (**Figure 6A**). Hippocampal BDNF content correlated significantly with mNSS scores (r = 0.608; P < 0.05). Plasma BDNF did not correlate with hippocampal BDNF (r = 0.517, P = 0.104), Caspase-3 (r = 0.283, P = 0.372), CA1 mean gray matter density (r = −0.064, P = 0.843), CA1 volume (r = 0.124, P = 0.613), mNSS (r = −0.04, P = 0.872), or Bcl-2/Bax (r = −0.45, P = 0.141).

Hippocampal TrkB correlated with hippocampal BDNF (r = 0.702, P < 0.05), apoptosis-related molecules (Caspase-3: r = −0.504, P < 0.05; Bcl-2/Bax: r = 0.52, P < 0.05), mean gray matter density of CA1 (r = −0.729, P < 0.01), and FA (r = 0.72, P < 0.01). However, plasma TrkB content did not correlate with FA value (r = −0.329, P = 0.297), CA1 volume (r = 0.178, P = 0.579), mean gray matter density of CA1 (r = −0.018, P = 0.957), mNSS score (r = 0.11, P = 0.743), Bcl-2/Bax (r = −0.34, P = 0.28), Caspase-3 (r = 0.266, P = 0.403), or hippocampal BDNF (r = −0.465, P = 0.15).

Correlations between MRI-related parameters and both apoptosis-related factors and mNSS

We performed linear correlation analyses between CA1 mean gray matter density, CA1 volume, and FA value, with mNSS, hippocampal Caspase-3 levels, and the Bcl-2/Bax ratio (**Figure 6B**). After GCI/RI, the CA1 volume and gray matter density differed from those of other subregions. Further, we found no differences in CA1 gray matter densities on days 3, 7, or 14 after reperfusion. Therefore, we only selected CA1 volume and gray matter density, as well as the hippocampal FA value, Caspase-3, Bcl-2/Bax ratio, and mNSS scores, for correlation analyses.

CA1 gray matter density correlated with Caspase-3 (r = 0.72, P < 0.01) and Bcl-2/Bax (r = −0.65, P < 0.05) levels. However, it did not correlate with mNSS (r = 0.37, P = 0.218). Similarly, CA1 volume correlated with Caspase-3 (r = 0.55, P < 0.05) and Bcl-2/Bax (r = −0.55, P < 0.05) levels but not mNSS score (r = 0.142, P = 0.509). FA correlated with Caspase-3 (r = −0.91, P < 0.01) and Bcl-2/Bax (r = 0.85, P < 0.01) levels, as well as mNSS (r = −0.61, P < 0.01).

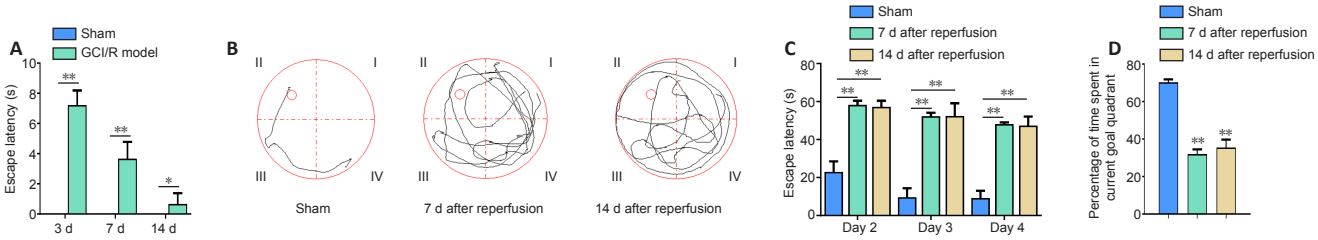

Figure 1 | **Change in mNSS and Morris water maze performance in GCI/RI rats.**
(A) Rat mNSS on days 3, 7, and 14 after GCI/RI in both groups. (B) Morris water maze trajectories (black lines). (C) Escape latencies over three consecutive days on the spatial navigation test. (D) Percentage of time spent in the goal quadrant during the space exploration test. Data are expressed as mean ± SD (n = 10). *P < 0.05, **P < 0.01, *vs.* sham group (Student's t-test). GCI/RI: Global cerebral ischemia/reperfusion injury; mNSS: modified neurological severity score.

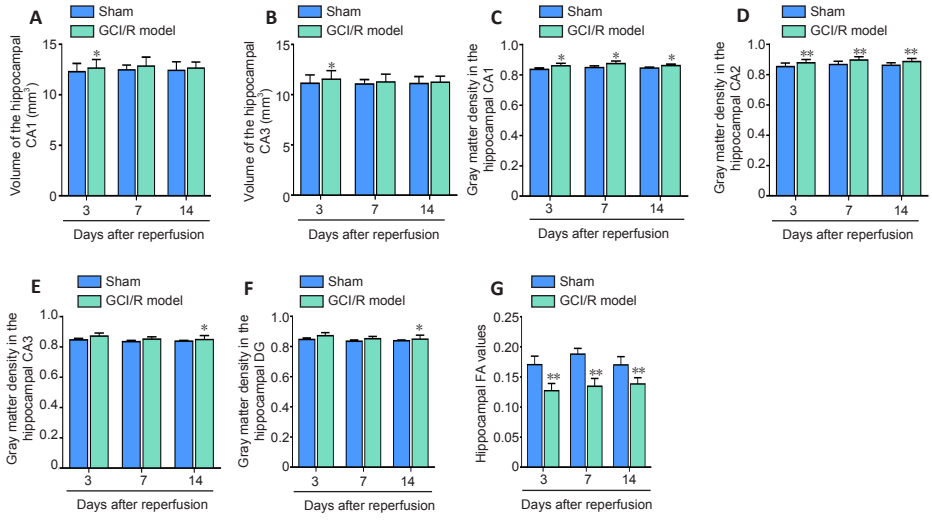

Figure 2 | **Hippocampal MRI findings 3, 7, and 14 days after GCI/RI.**
(A, B) Volumes of the hippocampal CA1 (A) and CA3 (B) areas. (C–F) Gray matter density of the hippocampal CA1 (C), and CA2 (D), CA3 (E) and DG (F) areas. (G) Hippocampal FA values. Data are expressed as mean ± SD (n = 5). *P < 0.05, **P < 0.01, *vs.* sham group (Student's t-test). DG: Dentate gyrus; FA: fractional anisotropy; GCI/RI: global cerebral ischemia/reperfusion injury.

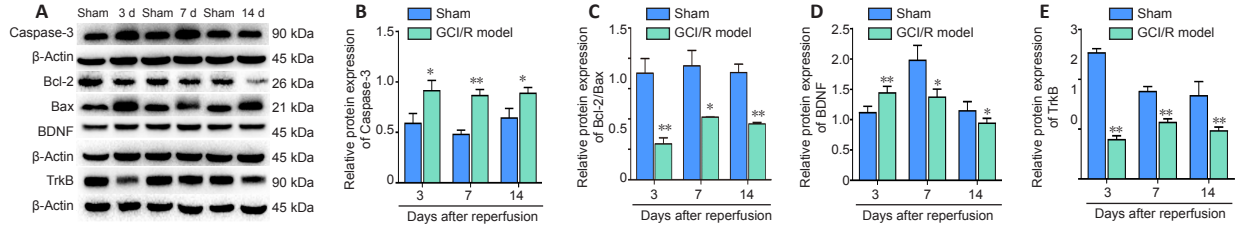

Figure 3 | **Apoptosis-related factors, BDNF, and TrkB expression levels in the hippocampus on days 3, 7, and 14 after GCI/RI.**
(A) Western blot bands. (B, D, E) Relative protein expression of Caspase-3, BDNF, and TrkB in the hippocampus. (C) Bcl-2/Bax ratio in the hippocampus. Data are expressed as mean ± SD (n = 6). *P < 0.05, **P < 0.01, *vs.* sham group (Student's t-test). BDNF: Brain-derived neurotrophic factor; GCI/RI: global cerebral ischemia/reperfusion injury; TrkB: tyrosine receptor kinase B.

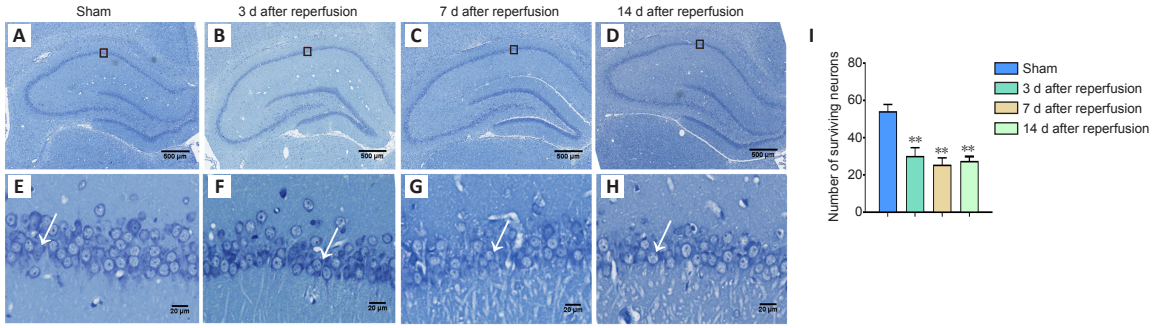

Figure 4 | **Nissl staining of the hippocampus on days 3, 7, and 14 after GCI/RI.**
(A–D) Nissl staining of the hippocampal CA1 area and the resulting findings on days 3, 7, and 14 after reperfusion injury. No differences were found in the mean number of pyramidal neurons in hippocampal CA1 at different time points. (E–H) Higher-resolution images of the red boxed regions in A–D. White arrows indicate Nissl-positive cells. Scale bars: 500 μm in A–D (low magnification photos), 20 μm in E–H. (I) Quantitative result of Nissl-positive cells in hippocampal CA1 area. Data are expressed as mean ± SD (n = 6). **P < 0.01, *vs.* sham group (Student's t-test). GCI/RI: Global cerebral ischemia/reperfusion injury.

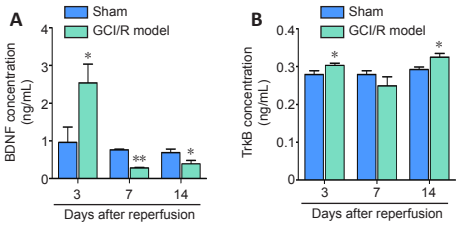

Figure 5 | Plasma BDNF and TrkB levels on days 3, 7, and 14 after GCI/RI.
BDNF (A) and TrkB (B) data were obtained by enzyme-linked immunosorbent assays. Data are expressed as mean ± SD (n = 6). *P < 0.05, *vs.* sham group (Student's t-test). BDNF: Brain-derived neurotrophic factor; GCI/RI: global cerebral ischemia/reperfusion injury; TrkB: tyrosine receptor kinase B.

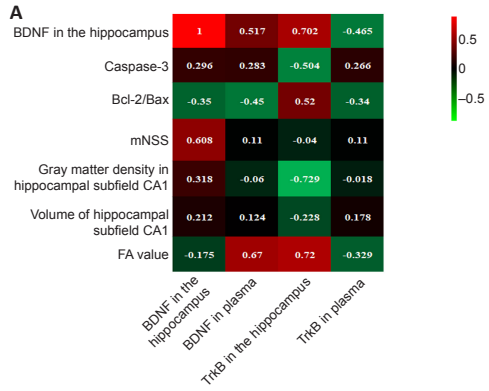

Figure 6 | Correlation results between hippocampal/plasma BDNF or TrkB levels with the degree of hippocampal injury after GCI/RI in rats.
(A) Linear correlation analysis of the heat map results for hippocampal and plasma BDNF and TrkB content, apoptosis-related molecules, mNSS score, and hippocampal MRI parameters. (B) Linear correlation analysis of hippocampal MRI parameters, apoptosis-related molecules, and mNSS. Each square shows the correlation between the variables on each axis. Red values indicate positive correlations, green indicate negative correlations, and black indicates no correlation. BDNF: Brain-derived neurotrophic factor; GCI/RI: global cerebral ischemia/reperfusion injury; TrkB: tyrosine receptor kinase B.

Discussion

Our findings revealed that plasma BDNF and TrkB levels were not correlated with mNSS after reperfusion. However, we observed a correlation between the hippocampal FA value and neurological function, Caspase-3, and Bcl-2/Bax. CA1 gray matter density correlated with Caspase-3. Our findings suggest that DTI-detectable alterations within the hippocampus reflect the severity of hippocampal injury induced by GCI/RI, not changes in plasma BDNF or TrkB levels.

Apoptosis is the main pathological mechanism underlying ischemic brain injury after delayed neuronal death in GCI/RI (Kalogeris et al., 2012). As an apoptosis regulator, Bcl-2 plays a diametrically opposing role to Bax and caspase-3 in apoptosis; it is a survival factor that can inhibit cell apoptosis and necrosis (Hockenbery et al., 1993). Apoptotic signals prompt Bax migration to mitochondria where it promotes apoptosis (Lalier et al., 2007). Therefore, the Bcl-2/Bax ratio determines the tendency of a cell toward apoptosis, with lower levels indicating greater apoptosis. Our findings revealed that the neurological severity scores at day 14 after GCI/RI were similar between experimental and sham groups. The hippocampal Bcl-2/Bax ratio and TrkB expression remained at low levels, while the Caspase-3 levels continued to increase and the number of hippocampal neurons continued to decrease. Therefore, the spatial learning and memory of rats with GCI/RI remained poor.

In some neurological diseases, decreased BDNF expression is associated with neuronal autophagy and death (Munno et al., 2013). Our results showed a decline in plasma BDNF levels after GCI/RI, which is consistent with the changes in plasma BDNF levels after stroke (Chaturvedi et al., 2020). BDNF binding to TrkB initiates dimerization and autophosphorylation of intracellular tyrosine residues to form phosphorylated TrkB, which stimulates various signaling pathways associated with the Rho family, including phosphatidylinositol 3-kinase, mitogen-activated protein kinase, phospholipase C-c, and guanosine triphosphate hydrolases. This activity further regulates calcium ion concentration, apoptosis, microfilament and microtubule growth, and dendritic spine formation. (Kowiański et al., 2018). Disturbance in BDNF synthesis or decreased TrkB expression can cause regulatory signaling pathway dysfunction, which could be a factor underlying multiple pathological processes.

Previous studies have reported an association of post-stroke neuronal damage or inflammation with decreased hippocampal BDNF and TrkB expression (Chen et al., 2015; Tanaka et al., 2018; Hsu et al., 2020). We observed that hippocampal BDNF expression was markedly higher on the 3rd day, but had decreased by the 7th day. There was a positive correlation between hippocampal BDNF and TrkB levels on days 7 and 14 after GCI/RI. Because BDNF can cross the blood-brain barrier, peripheral and brain BDNF levels are expected to be related (Waterhouse and Xu, 2009; Munno et al., 2013; Lu et al., 2015), which is consistent with our findings. After GCI/RI, we observed a positive correlation between plasma and hippocampal BDNF levels. Conversely, and inconsistent with previous reports of a correlation between blood TrkB levels and brain damage (Munno et al., 2013; Yang et al., 2020), we observed no correlation between hippocampal or plasma TrkB levels with neurological severity scores after GCI/RI. Although the brain is the main BDNF source in humans, BDNF can also be produced by vascular endothelial cells, T cells, B cells, monocytes, the heart, lungs, ovaries, kidneys, peripheral nerves, and other peripheral tissue cells, which affects peripheral BDNF levels (Lee et al., 2018; Tian et al., 2019). Therefore, although there is some correlation between plasma and hippocampal BDNF levels, the correlation coefficient is low.

TrkB is primarily expressed in the plasma membrane (Zahavi et al., 2018) and is a high-affinity receptor for BDNF, neurotrophin-4, and neurotrophin-3 (Gao et al., 1995). Moreover, TrkB is highly expressed in the central nervous system, as well as in peripheral mononuclear cells (Yang et al., 2020). The source of TrkB in plasma is more complicated than that of BDNF, with more factors regulating changes in TrkB expression. Therefore, although there are post-GCI/RI changes in plasma TrkB levels, these changes are inconsistent with changes in hippocampal TrkB expression. Further, they cannot reflect the degree of hippocampal injury or post-reperfusion neurological damage.

MRI-related parameters are highly correlated with the loss of neuronal function. Specifically, the hippocampal FA value and mean gray matter density of the CA1 subregion. A previous study reported that BDNF content was positively correlated with FA values and hippocampal white matter integrity (Chen et al., 2016). We found that hippocampal FA values had decreased on days 7 and 14 after GCI/RI, with plasma and hippocampal BDNF levels showing a corresponding decrease. The various hippocampal subfields show different responses

to ischemia/reperfusion injury (Butler et al., 2010). Given that glutamate receptors are more densely distributed in CA1 pyramidal cells (Butler et al., 2010), and that ROS production is more difficult to control in CA1 than in CA3 (Yin et al., 2017), CA1 is the most sensitive hippocampal region to ischemia, with its volume and gray matter density showing the most rapid changes after GCI/RI. However, studies on Alzheimer's disease have reported no correlation between plasma BDNF levels and hippocampal volume or memory (Kim et al., 2015). In conclusion, we investigated the correlation of plasma BDNF and TrkB levels with post-GCI/RI hippocampal injury. Although plasma TrkB expression levels did not reflect the degree of hippocampal injury, hippocampal FA values and the mean gray matter density in CA1 did reflect neuronal functional status and hippocampal damage to some extent. This study provides novel evidence regarding the relationship between GCI/RI and the BDNF/TrkB pathway. Moreover, it suggests an objective indicator for the degree of brain damage suffered after ischemia/reperfusion injury and provides a basis for further treatment and decision-making. Although we found no correlation between plasma and hippocampal TrkB levels after GCI/RI, additional studies should determine whether TrkB levels in plasma is related to other factors. Moreover, extensive research is needed on the correlation of plasma BDNF levels with the degree of hippocampal damage after reperfusion injury. We aim to conduct additional studies to answer these questions.

Author contributions: *Study concept and design, manuscript writing and language polishing: HTL, WZW; experiment implementation: WZW, XL, YZW; data analysis: XL, ZYY, WZW. All authors read and approved the final manuscript.*
Conflicts of interest: *The authors declare that they have no conflict of interests.*
Financial support: *This study was supported by the Fundamental Research Funds for Central Public Welfare Research Institute of China, Nos. 2015CZ-36 (to HTL) and 2019CZ-7 (to WZW). The funding sources had no role in study conception and design, data analysis or interpretation, paper writing or deciding to submit this paper for publication.*
Institutional review board statement: *This study was approved by the Institutional Animal Care and Use Committee of Capital Medical University (approval No. AEEI-2015-139) on November 9, 2015.*

Data sharing statement: *Datasets analyzed during the current study are available from the corresponding author on reasonable request.*
Plagiarism check: *Checked twice by iThenticate.*
Peer review: *Externally peer reviewed.*

Open peer reviewers: *Saritha Krishna, University of California San Francisco, USA; Audrey D Lafrenaye, Virginia Commonwealth University, USA.*
Additional file: *Open peer review reports 1 and 2.*

References

Ashburner J (2012) SPM: a history. Neuroimage 62:791-800.
Béjot Y, Mossiat C, Giroud M, Prigent-Tessier A, Marie C (2011) Circulating and brain BDNF levels in stroke rats. Relevance to clinical studies. PLoS One 6:e29405.
Butler TR, Self RL, Smith KJ, Sharrett-Field LJ, Berry JN, Littleton JM, Pauly JR, Mulholland PJ, Prendergast MA (2010) Selective vulnerability of hippocampal cornu ammonis 1 pyramidal cells to excitotoxic insult is associated with the expression of polyamine-sensitive N-methyl-D-asparate-type glutamate receptors. Neuroscience 165:525-534.
Callaghan CK, Kelly ÁM (2012) Differential BDNF signaling in dentate gyrus and perirhinal cortex during consolidation of recognition memory in the rat. Hippocampus 22:2127-2135.
Chaturvedi P, Singh AK, Tiwari V, Thacker AK (2020) Brain-derived neurotrophic factor levels in acute stroke and its clinical implications. Brain Circ 6:185-190.
Chen HH, Zhang N, Li WY, Fang MR, Zhang H, Fang YS, Ding MX, Fu XY (2015) Overexpression of brain-derived neurotrophic factor in the hippocampus protects against post-stroke depression. Neural Regen Res 10:1427-1432.
Chen J, Niu Q, Xia T, Zhou G, Li P, Zhao Q, Xu C, Dong L, Zhang S, Wang A (2018) ERK1/2-mediated disruption of BDNF-TrkB signaling causes synaptic impairment contributing to fluoride-induced developmental neurotoxicity. Toxicology 410:222-230.
Chen NC, Chuang YC, Huang CW, Lui CC, Lee CC, Hsu SW, Lin PH, Lu YT, Chang YT, Hsu CW, Chang CC (2016) Interictal serum brain-derived neurotrophic factor level reflects white matter integrity, epilepsy severity, and cognitive dysfunction in chronic temporal lobe epilepsy. Epilepsy Behav 59:147-154.
Elfving B, Plougmann PH, Wegener G (2010) Detection of brain-derived neurotrophic factor (BDNF) in rat blood and brain preparations using ELISA: pitfalls and solutions. J Neurosci Methods 187:73-77.
Fletcher E, Gavett B, Harvey D, Farias ST, Olichney J, Beckett L, DeCarli C, Mungas D (2018) Brain volume change and cognitive trajectories in aging. Neuropsychology 32:436-449.
Fujioka M, Okuchi K, Sakaki T, Hiramatsu K, Miyamoto S, Iwasaki S (1994) Specific changes in human brain following reperfusion after cardiac arrest. Stroke 25:2091-2095.
Gao WQ, Zheng JL, Karihaloo M (1995) Neurotrophin-4/5 (NT-4/5) and brain-derived neurotrophic factor (BDNF) act at later stages of cerebellar granule cell differentiation. J Neurosci 15:2656-2667.
Herrmann FR, Rodriguez C, Haller S, Garibotto V, Montandon ML, Giannakopoulos P (2019) Gray matter densities in limbic areas and APOE4 independently predict cognitive decline in normal brain aging. Front Aging Neurosci 11:157.
Hockenbery DM, Oltvai ZN, Yin XM, Milliman CL, Korsmeyer SJ (1993) Bcl-2 functions in an antioxidant pathway to prevent apoptosis. Cell 75:241-251.
Hsu CC, Kuo TW, Liu WP, Chang CP, Lin HJ (2020) Calycosin preserves BDNF/TrkB signaling and reduces post-stroke neurological injury after cerebral ischemia by reducing accumulation of hypertrophic and TNF-α-containing microglia in rats. J Neuroimmune Pharmacol 15:326-339.
Jakaria M, Park SY, Haque ME, Karthivashan G, Kim IS, Ganesan P, Choi DK (2018) Neurotoxic agent-induced injury in neurodegenerative disease model: focus on involvement of glutamate receptors. Front Mol Neurosci 11:307.
Kalogeris T, Baines CP, Krenz M, Korthuis RJ (2012) Cell biology of ischemia/reperfusion injury. Int Rev Cell Mol Biol 298:229-317.
Kim A, Fagan AM, Goate AM, Benzinger TL, Morris JC, Head D (2015) Lack of an association of BDNF Val66Met polymorphism and plasma BDNF with hippocampal volume and memory. Cogn Affect Behav Neurosci 15:625-643.
Kowiański P, Lietzau G, Czuba E, Waśkow M, Steliga A, Moryś J (2018) BDNF: a key factor with multipotent impact on brain signaling and synaptic plasticity. Cell Mol Neurobiol 38:579-593.
Lalier L, Cartron PF, Juin P, Nedelkina S, Manon S, Bechinger B, Vallette FM (2007) Bax activation and mitochondrial insertion during apoptosis. Apoptosis 12:887-896.
Lee HW, Ahmad M, Weldrick JJ, Wang HW, Burgon PG, Leenen FHH (2018) Effects of exercise training and TrkB blockade on cardiac function and BDNF-TrkB signaling postmyocardial infarction in rats. Am J Physiol Heart Circ Physiol 315:H1821-1834.
Li K, Shen S, Ji YT, Li XY, Zhang LS, Wang XD (2018) Melatonin augments the effects of fluoxetine on depression-like behavior and hippocampal BDNF-TrkB signaling. Neurosci Bull 34:303-311.
Lu H, Zhang T, Wen M, Sun L (2015) Impact of repetitive transcranial magnetic stimulation on post-stroke dysmnesia and the role of BDNF Val66Met SNP. Med Sci Monit 21:761-768.
Munno D, Sterpone S, Fania S, Cappellin F, Mengozzi G, Saroldi M, Bechon E, Zullo G (2013) Plasma brain derived neurotrophic factor levels and neuropsychological aspects of depressed patients treated with paroxetine. Panminerva Med 55:377-384.
Planche V, Ruet A, Coupé P, Lamargue-Hamel D, Deloire M, Pereira B, Manjon JV, Munsch F, Moscufo N, Meier DS, Guttmann CR, Dousset V, Brochet B, Tourdias T (2017) Hippocampal microstructural damage correlates with memory impairment in clinically isolated syndrome suggestive of multiple sclerosis. Mult Scler 23:1214-1224.
Radhakrishnan H, Stark SM, Stark CEL (2020) Microstructural alterations in hippocampal subfields mediate age-related memory decline in humans. Front Aging Neurosci 12:94.
Tanaka N, Cortese GP, Barrientos RM, Maier SF, Patterson SL (2018) Aging and an immune challenge interact to produce prolonged, but not permanent, reductions in hippocampal L-LTP and mBDNF in a rodent model with features of delirium. eNeuro 5:ENEURO.0009-0018.2018.
Tian B, Yang C, Wang J, Hou X, Zhao S, Li Y, Yang P (2019) Peripheral blood brain-derived neurotrophic factor level and tyrosine kinase B expression on T lymphocytes in systemic lupus erythematosus: Implications for systemic involvement. Cytokine 123:154764.
Wang W, Liu X, Lu H, Liu L, Wang Y, Yu Y, Zhang T (2019) A method for predicting the success of Pulsinell's four-vessel occlusion rat model by LDF monitoring of cerebral blood flow decline. J Neurosci Methods 328:108439.
Wang W, Liu X, Yang Z, Shen H, Liu L, Yu Y, Zhang T (2020) Levodopa improves cognitive function and the deficits of structural synaptic plasticity in hippocampus induced by global cerebral ischemia/reperfusion injury in rats. Front Neurosci 14:586321.
Waterhouse EG, Xu B (2009) New insights into the role of brain-derived neurotrophic factor in synaptic plasticity. Mol Cell Neurosci 42:81-89.
Yang J, Tan J, Zheng L, Lu CX, Hou WQ, Liu Y, Li QF, Li JX, Cheng D, Luo X, Zhang J (2020) Plasma BDNF and TrkB mRNA in PBMCs are correlated with anti-depressive effects of 12-weeks supervised exercise during protracted methamphetamine abstinence. Front Mol Neurosci 13:20.
Yin B, Barrionuevo G, Batinic-Haberle I, Sandberg M, Weber SG (2017) Differences in reperfusion-induced mitochondrial oxidative stress and cell death between hippocampal CA1 and CA3 subfields are due to the mitochondrial thioredoxin system. Antioxid Redox Signal 27:534-549.
Zahavi EE, Steinberg N, Altman T, Chein M, Joshi Y, Gradus-Pery T, Perlson E (2018) The receptor tyrosine kinase TrkB signals without dimerization at the plasma membrane. Sci Signal 11:eaao4006.
Zhou Z, Lu T, Xu G, Yue X, Zhu W, Ma M, Liu W, Zhu S, Liu X (2011) Decreased serum brain-derived neurotrophic factor (BDNF) is associated with post-stroke depression but not with BDNF gene Val66Met polymorphism. Clin Chem Lab Med 49:185-189.

P-Reviewers: Krishna S, Lafrenaye AD; C-Editor: Zhao M; S-Editors: Yu J, Li CH; L-Editors: Yu J, Song LP; T-Editor: Jia Y